Available online at www.sciencedirect.com

ScienceDirect

Materials and Design 28 (2007) 1953–1957

Materials & Design

www.elsevier.com/locate/matdes

Short communication

Effect of traverse speed on abrasive waterjet machining of Ti–6Al–4V alloy

Ahmet Hascalik [a,*], Ulaş Çaydaş [a], Hakan Gürün [b]

[a] University of Firat, Technical Education Faculty, Department of Manufacturing, Elazig, Turkey
[b] University of Gazi, Technical Education Faculty, Department of Manufacturing, Ankara, Turkey

Received 3 August 2005; accepted 21 April 2006
Available online 16 June 2006

Abstract

In the presented study, Ti–6Al–4V alloy, known as one of the difficult-to-machine materials using conventional machining processes, was machined under varying traverse speeds of 60, 80, 120, 150, 200, and 250 mm/min by abrasive waterjet (AWJ) machining. After machining, the profiles of machined surfaces, kerf geometries and microstructural features of the machined surfaces were examined using surface profilometry and scanning electron microscopy (SEM). The experimental results indicate that the traverse speed of the jet is a significant parameter on the surface morphology, and the widths and features of different regions formed in the cutting surface change according to the traverse speed. It was also observed that the kerf taper ratio and surface roughness increase with increasing traverse speed in chosen conditions.

Keywords: AWJM; Jet traverse speed; Ti–6Al–4V

1. Introduction

Titanium and its alloys have excellent corrosion resistance, a high strength-to-weight ratio and good high temperature properties. Among several alloying types of titanium, Ti–6Al–4V is commonly used for space and aircraft applications, as well as high performance automotive and marine applications that require materials with high corrosion resistance and strength [1,2]. Titanium and its alloys are difficult-to-machine materials by conventional machining processes owing to several inherent properties of the material. Titanium is a highly chemically reactive element with almost all cutting tool materials, its low thermal conductivity and low modules of elasticity also impair machinability [3]. The main difficulties in machining them are high cutting temperatures and rapid tool wear. In the open literature, many authors have attempted to machine these materials with different cutting tools like straight grade cemented carbides (Wo–Co), polycrystalline diamond (PCD), and cubic boron nitride (CBN) [4,5]. According to these researches, it is pointed out that the cutting speeds and tool life are limited to a specific value. None of these tool materials, however, seems to be effective in machining titanium because of their chemical affinities with titanium.

Additionally, some non-traditional processes such as electrical discharge machining (EDM) [6] and laser machining (LM) [7] are also not an effective solution due to surface quality and heat affected zone.

Abrasive waterjet machining technology is one of the most recent non-traditional methods used in the industry for material processing with the distinct advantages of no thermal distortion, high machining versatility, high flexibility and small cutting forces [8,9]. Since there is not any electrical or thermal energy used in this process, many material defects can be ignored. Compared with traditional and

* Corresponding author. Tel.: +90 424 2370000x6544; fax: +90 424 2184674.
E-mail address: ahascalik@firat.edu.tr (A. Hascalik).

0261-3069/$ - see front matter © 2006 Elsevier Ltd. All rights reserved.
doi:10.1016/j.matdes.2006.04.020

non-traditional machining technologies, abrasive waterjet (AWJ) machining has been used increasingly with extensive applications for the shape cutting of difficult-to-machine materials such as Ti alloys. Besides, the process is more economical and the material removal rate (MRR) is higher than those of non-traditional machining processes.

In AWJ machining, the workpiece material is removed by the action of high-speed water mixed with abrasive particles. A high-speed waterjet transfers kinetic energy to the abrasive particles and the mixture impinges on to the workpiece [10]. The material removal rate is dependent on the abrasive attack and mechanical properties of target metal. The AWJ machining process is defined by a number of parameters, which in turn govern the material removal rate and the development of the characteristics of the surface. A considerable effort was made in understanding the influence of the system operational process parameters such as waterjet pressure, abrasive flow rate, standoff distance, number of passes on depth of cut, angle of cutting, and traverse speed [11–14]. The results of the studies showed that the AWJ machining is significantly affected by the variation of process parameters. However, the degree of influence of parameters depends on the magnitude of parametric variation and machinability of the material. Traverse speed of the jet has a strong influence on the surface finish of the workpiece and material removal rate. Ojmertz [15] has shown that low traverse speeds result in an irregular surface morphology and significantly increased material removal rates but despite this, lower surface roughness values are observed. Fowler et al. [16] have shown that low jet traverse speed not only results in high material removal rates, but also in high surface waviness.

The aim of this study is to investigate experimentally the profiles of machined surfaces, kerf geometries and microstructural features of the machined surfaces in terms of traverse speed in AWJ-machined Ti–6Al–4V alloy.

2. Experimental procedure

The material used in this study was commercial Ti–6Al–4V with a thickness of 4.87 mm. The nominal chemical compositions of the test material are listed in Table 1. The experiments were performed on a WSI (Waterjet Service Inc.) model WA50 High-Pressure Waterjet machine. In the experiments, traverse speeds of 60, 80, 120, 150, 200, and 250 mm/min were used. Pressure (150 MPa), jet impact angle (90°), grit mesh number of garnet (80), abrasive flow rate (0.005 kg s^{-1}), and standoff (3 mm) were fixed. After machining, the microstructures of cutting surfaces were observed by scanning electron microscopy (SEM). Average surface roughnesses (R_a) were measured at 1 mm spacings from the jet entry to exit by a Mitutoyo Surftest SJ-201 portable device. The kerf wideness and depth of SCR were measured using a stereo zoom microscope.

Table 1
Chemical composition of specimens (wt%)

Ti	Al	V	Fe	O	C	N	H
89.464	6.08	4.02	0.22	0.18	0.02	0.01	0.0053

3. Experimental results and discussion

3.1. Surface morphology

Fig. 1 shows cutting surface view of samples machined at traverse speed of 60–200 mm/min, respectively. Microstructural evaluation of the cutting surfaces of samples revealed three distinct zones which were identified as: (1) a initial damage region (IDR), which is cutting zone at shallow angles of attack; (2) a smooth cutting region (SCR), which is cutting zone at large angles of attack; (3) a rough cutting region (RCR), which is the jet upward deflection zone [17,18]. The surface morphology in different regions of cutting surface is generated from the instantaneous penetration of abrasive waterjet. It is expected that these regions would change with an increasing interaction of the jet with the material, i.e., increased overlap at any region of cut. As can be seen from the figures, as the traverse speed increases, the number of particles impinging on a given exposed target area decreases, which in turn reduces the IDR width slightly. The width of SCR also decreases with the increase of traverse speed, because the depth of penetration decreases. Scanning electron microscopy analysis of the cutting surface texture revealed that

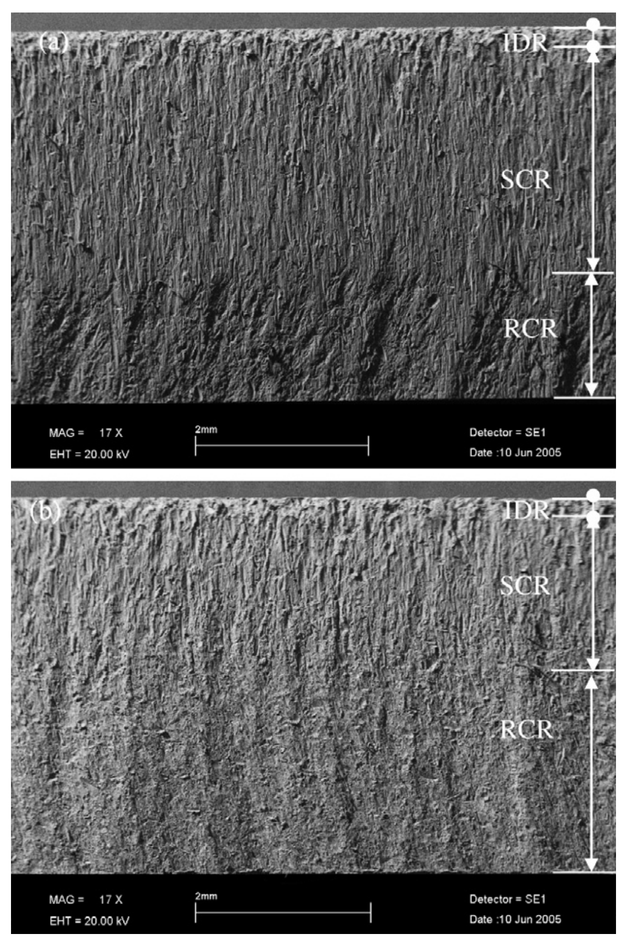

Fig. 1. Typical AWJ-machined surface: (a) for traverse speed of 60 mm/min and (b) for traverse speed of 200 mm/min.

the mechanism of material removal was a combination of scooping induced ductile shear and ploughing actions of the abrasive particles. In a previous study, it was claimed that the cutting mechanism in the IDR and SCR could be considered as cutting wear and deformation wear, respectively, while in the RCR the cutting process is considered as being controlled by erosive wear at large particle attack angles [19]. The degree of plastic deformation increases from the top to the bottom of the cutting surfaces. Typical microstructures from these regions are shown in Figs. 2–4. In the IDR of the cutting surface, abrasive particles have a sufficient level of kinetic energy to destruct the material. This small damaged region is characterized by a small rounded corner at the top edge due to the plastic deformation of material caused by the initial AWJ bombardment. As the abrasive particles penetrate into the material, some of the energy is used in eroding the material in the SCR and the stream loses kinetic energy. A jet with lower energy tends to deflect in the normal direction to the plane of cutting, which will result in striations to be formed on the cutting surface. As the abrasive jet stream traverses the part, the stream is deflected, hence resulting in the creation of a unique cutting geometry. The degree of deflection increases with increasing traverse speed. Arola and Ramulu [20] also suggest that striation formation is a result of reduction in the jet energy. According to other reported studies, three major sources contribute to the striation formation simultaneously, i.e., the nature of the step formation cutting process, the waterjet dynamic characteristics, and the machine system vibration [21].

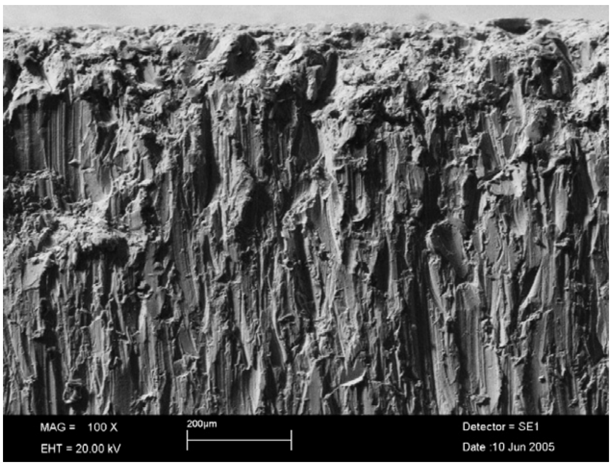

Fig. 2. SEM micrograph of IDR.

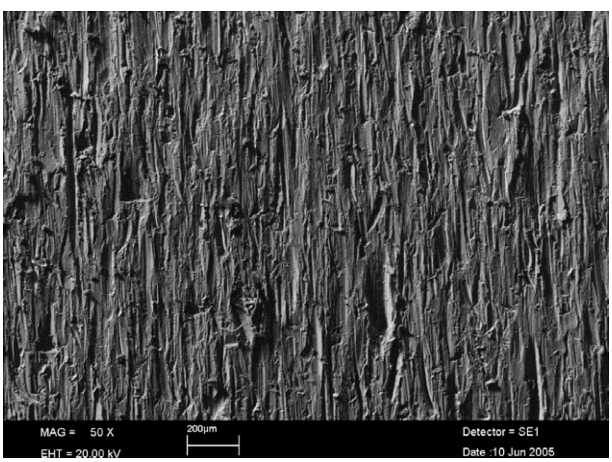

Fig. 3. SEM micrograph of SCR.

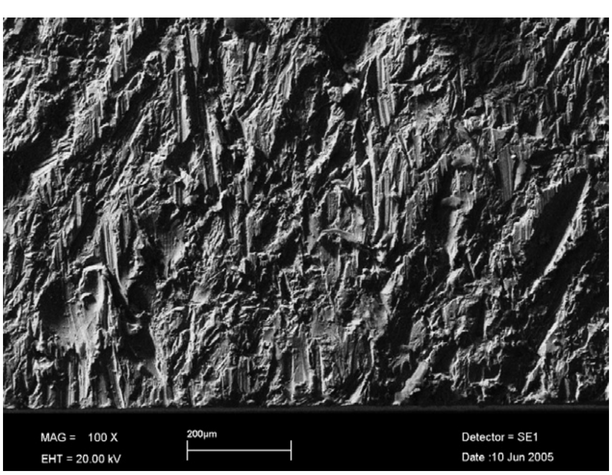

Fig. 4. SEM micrograph of RCR.

3.2. Kerf geometry

The kerf taper angle for each cut was calculated using the measured values of the top and bottom kerf width for each cut based on the equation

$$\theta = \arctan[(W_t - W_b)/(2xt)], \quad (1)$$

where t is the material thickness. Kerf geometry is a characteristic of major interest in abrasive waterjet process. The top kerf is commonly wider than the bottom due to the de-

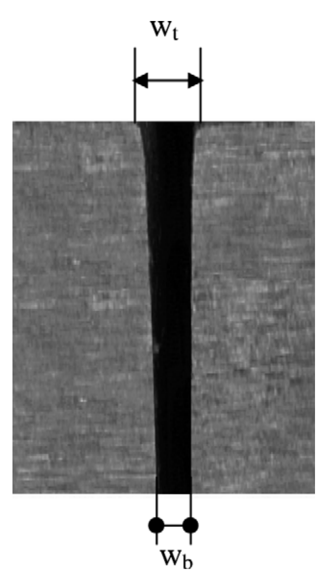

Fig. 5. A typical side view of the kerf (W_t: top kerf width; W_b: bottom kerf width).

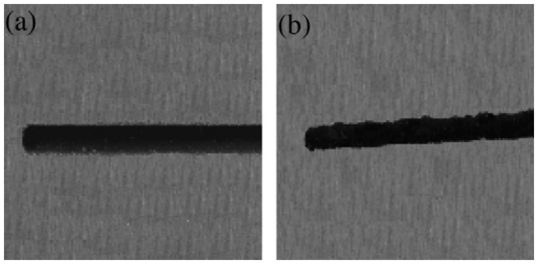

Fig. 6. A view of jet entry (a) and jet exit (b).

crease in water pressure as a unique feature of AWJ technology. As a result of this, a taper is produced. The large kerf taper ratio worsens the perpendicularity or the straightness of the cutting cross-section, resulting in an inaccurate dimensional quality. A typical side view of the kerf is shown in Fig. 5, while jet entry and exit of the workpiece are shown in Fig. 6. As traverse speed increases, top and bottom kerf widths decrease, but despite this, kerf wall slope increases slightly. This is because the traverse speed of abrasive waterjet allows fewer abrasives to strike on the jet target and hence generates a narrower slot.

As the traverse speed increases, the AWJ cuts narrower kerf widths with a greater kerf taper ratio, as shown in Fig. 7. Although the kerf taper ratio is differs for increasing traverse speed, this change is only 0.54° for the tested specimens.

3.3. Surface roughness and the depth of SCR

Fig. 8 shows surface roughness versus depth of measurement with respect to traverse speed. As seen from this figure, the surface roughness is approximately constant as the depth of the cut gets deeper in SCR. After that, the surface quality deteriorates because the jet loses its energy due to the jet–material interaction and mutual particle impacts. Additionally, the jet impact angle worsens perpendicularly and in RCR, the deformation wear mechanism becomes more effective than the top of the cutting region where the cutting wear mechanism is dominant. From the experimental results, it can be noticed that an increase in the traverse speed causes a constant increase in the surface

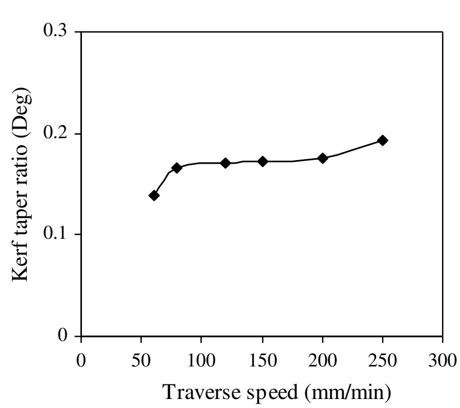

Fig. 7. Effect of traverse speed on kerf taper ratio.

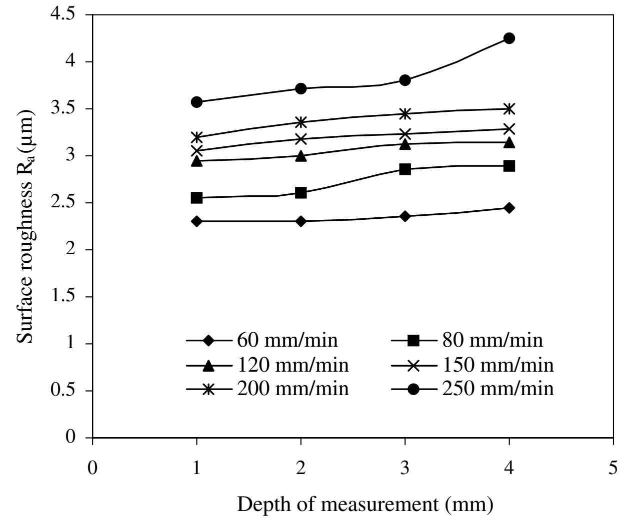

Fig. 8. Surface roughness versus depth of measurement for different traverse speeds.

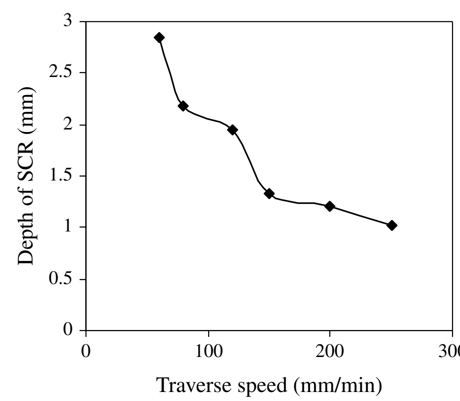

Fig. 9. The depth of smooth cutting regions for different traverse speeds.

roughness. This may be anticipated as increasing traverse speed allows less overlap machining action and fewer abrasive particles to impinge the surface, increasing the roughness of the surface [22]. Surface roughness values (R_a) were measured as 2.30–3.57 µm at the same measurement depth (1 mm from the jet entry) in the traverse speed of 60–250 mm/min, respectively. This indicates that the surface roughness increment amount is about 1.27 µm in SCR. Consequently, the traverse speed may be selected in high values in terms of machining time, unless the surface roughness is of a major concern.

The depth of the cut and the smooth cutting region are two major characteristics in AWJ process. While the depth of the cut represents the capacity of the jet to penetrate into the material, the depth of SCR ideally equal to the total cutting surface area is always desirable. Generally, the smooth cutting region is taken as the average surface quality. Fig. 9 shows the depth of smooth cutting regions for different traverse speeds. With increasing traverse speed, the smooth cutting region depth of samples decreases. At high traverse speed, the SCR decreased to about 25% of the total cutting surface area, while this ratio is about

60% at low traverse speed. Hence, the traverse speed appears to be the significant parameter on a depth of the SCR.

4. Conclusions

In this study, the profiles of machined surfaces, kerf geometries and microstructural features of the machined surfaces in terms of traverse speed in AWJ-machined Ti–6Al–4V alloy were investigated experimentally. Summarizing the main features of the results, the following conclusions may be drawn:

1. Microstructural evaluation of the cutting surfaces of samples revealed three distinct zones which were identified as: (1) an initial damage region (IDR), which is cutting zone at shallow angles of attack; (2) a smooth cutting region (SCR), which is cutting zone at large angles of attack; (3) a rough cutting region (RCR), which is the jet upward deflection zone.
2. As the traverse speed increases, the AWJ cuts narrower kerf widths with a greater kerf taper ratio. This is because the traverse speed of abrasive waterjet allows fewer abrasives to strike on the jet target and hence generates a narrower slot. Although the kerf taper ratio differs for increasing traverse speed, this change is only 0.54° for the tested specimens.
3. The surface roughness is approximately constant, as the depth of the cut gets deeper in SCR. After that, the surface quality deteriorates because the jet loses its energy due to the jet–material interaction, and mutual particle impacts.
4. With increasing traverse speed, the smooth cutting region depth of samples decreases. At high traverse speed, the SCR decreased to about 25% of the total cutting surface area, while this ratio is about 60% at low traverse speed. Hence, the traverse speed appears to be a significant parameter on the depth of the SCR.

References

[1] Barry J, Byrne G, Lennon D. Observations on chip formation and acoustic emission in machining Ti–6Al–4V alloy. Int J Mach Tools Manuf 2001;41:2245–60.

[2] Hong SY, Markus I, Jeong W. New cooling approach and tool life improvement in cryogenic machining of titanium alloy Ti–6Al–4V. Int J Mach Tools Manuf 2001;41:1055–70.

[3] Ezugwu EO, Wang ZM. Titanium alloys their machinablity – a review. J Mater Process Technol 1997;68(3):262–74.

[4] Nabbani F. Machining of aerospace titanium alloys. Robot Com Int Manuf 2001;17:99–106.

[5] Zoya ZA, Krishnamurthy R. The performance of CBN tools in the machining of titanium alloys. J Mater Process Technol 2000;100: 80–6.

[6] Chen SL, Yan BH, Huang FY. Influence of kerosene and distilled water as dielectrics on the electric discharge machining characteristics of Ti–6Al–4V. J Mater Process Technol 1999;87:107–11.

[7] Bandyopadhyay S, Sarin S, Sundararajan JK, Joshi G. Geometrical features and metallurgical characteristics of Nd:YAG laser drilled holes in thick IN718 and Ti–6Al–4V sheets. J Mater Process Technol 2002;127:83–95.

[8] Akkurt A, Kulekci MK, Seker U, Ercan F. Effect of feed rate on surface roughness in abrasive waterjet applications. J Mater Process Technol 2004;147:389–96.

[9] Van Luttervelt CA. On the selection of manufacturing methods illustrated by an overview of separation techniques for sheet materials. Ann CIRP 1989;38(2):587–607.

[10] Seo YW, Ramulu M, Kim D. Machinability of titanium alloy (Ti–6Al–4V) by abrasive waterjets. Proc Instn Mech Eng B 2003;217: 1709–21.

[11] Hashish M. A modelling study of metal cutting with abrasive waterjets. J Eng Mater Technol 1984;106:88–100.

[12] Arola D, Ramulu M. Mechanism of material removal in abrasive waterjet machining of common aerospace materials. In: Proceedings of the seventh American waterjet conference. Seattle (WA); 1993. p. 43–64.

[13] Hashish M. Optimization factors in abrasive waterjet machining. ASME J Eng Ind 1991;113:9–37.

[14] Blickwedel H, Guo NS, Haferkamp H, Louis H. Prediction of abrasive jet cutting performance and quality. Jet Cutting Technol 1991:163–79.

[15] Ojmertz KMC. Abrasive waterjet milling: an experimental investigation. In: Hashish M, editor. Proceedings of the seventh US water jet conference. St. Louis: Water Jet Technical Association; 1993. p. 777–91.

[16] Fowler G, Shipway PH, Pashby IR. Abrasive water-jet controlled depth milling of Ti–6Al–4V alloy – an investigation of the role of jet-workpiece traverse speed and abrasive grit size on the characteristics of the milled material. J Mater Process Technol 2005;161:407–24.

[17] Seo YW, Ramulu M, Kim D. Machinability of titanium alloy (Ti–6Al–4V) by abrasive waterjets. Proc Instn Mech Eng B 2003(217).

[18] Wang J. Abrasive waterjet machining of polymer matrix composites: cutting performance erosive analysis and predictive models. Int J Adv Manufact Technol 1999;15:757–68.

[19] Wang J. A machinability study of polymer matrix composites using abrasive waterjet cutting technology. J Mater Process Technol 1999;94(1):30–45.

[20] Arola D, Ramulu M. Material removal in abrasive waterjet machining of metals surface integrity and texture. Wear 1997(210):50–8.

[21] Guo NS, Louis G, Meier G. Surface structure and kerf geometry in abrasive waterjet cutting: formation and optimization. In: Proceedings of the seventh American waterjet conference, Seattle (WA, USA); 1993.

[22] L Chen F, Wang J, Lemma E, Siores E. Striation formation mechanism on the jet cutting surface. J Process Technol 2003;141: 213–8.